

## LASER-COMPTON SCATTERING AS A POTENTIAL BRIGHT X-RAY SOURCE

K. Chouffani<sup>1</sup>, D. Wells<sup>1</sup>, F. Harmon<sup>1</sup>, G. Lancaster<sup>2</sup>, J. Jones<sup>2</sup>

<sup>1</sup>*Idaho Accelerator Center, 1500 Alvin Ricken DR., Pocatello, ID 83209, USA*

<sup>2</sup>*Idaho National Engineering and Environmental Laboratory, P.O. Box 1625, MS 2802, Idaho Falls, ID 83415-2802, USA*

### ABSTRACT

Laser-Compton scattering (LCS) experiments were carried out at the Idaho Accelerator Center (IAC). Sharp monochromatic X-ray lines were observed which result from the interaction of the electron beam with the laser optical photons. The back-scattered photons are kinematically boosted to keV X-ray energies. The X-rays were generated by colliding a 20-22 MeV, 5-20 ns electron beam with a 100 MW, 7 ns Nd:YAG laser. We observed low background, sharp LCS X-ray spectral peaks resulting from the interaction of the electron beam with the Nd:YAG laser fundamental and second harmonic lines (1064 and 532 nm). The LCS X-ray energy lines and energy deviations were measured as a function of the electron beam energy and energy-spread respectively. The experimental results showed good agreement with the predicted values. Because LCS X-rays are monochromatic, with energies that are easily tunable, have the same polarization as the laser, and the same time structure as that of the electron beam, LCS could be used as a unique X-ray source with a broad range of applications.

### INTRODUCTION

There is great industrial and scientific interest in bright, monochromatic and tunable X-ray sources. These sources are being widely used in various scientific research fields as well as in medical [1,2], technology [3], and industrial [4] fields. Synchrotron radiation (SR) is currently the primary, high-quality X-ray source that satisfies both brilliance and tenability. The high cost, large size, and low x-ray energies of SR facilities, however, are serious limitations. With the advent of new linear accelerator (LINAC) technology, the potential for new, compact, and inexpensive X-ray sources has never been greater.

There have been several experimental and theoretical works devoted to exotic X-ray sources using electron beam interaction with periodic structures (EIPS) [5-7]. These coherent and monochromatic sources can produce fast X-ray pulses with energies ranging from 2 to 100 keV (for a 20 MeV electron beam). Unfortunately, these sources suffer from a modest photon flux and are limited by the damage threshold of the target from high electron beam current and multiple scattering inside the target.

Recent results and publications [8-10] have shown that laser Compton scattering by relativistic electrons can produce ultra fast, directional, quasi-monochromatic, and polarized photon beams with intensity orders of magnitude higher than the X-ray sources mentioned above.

LCS is the exchange of energy between relativistic electron and laser beams. When photons interact with high energy moving electrons (in the MeV region), the electrons scatter low energy photons to a higher energy at the expense of the electrons' kinetic energy. This interaction results in the emission of highly directed (peaked in the direction of the incident electron beam), mono-energetic (see below), highly polarized and tunable X-ray beams with a divergence on the order of  $1/\gamma$ , where  $\gamma$  is the ratio of electron total energy over the electron rest energy.

## EXPERIMENT

LCS kinematics has been discussed in elsewhere [10-12]. The backscattered x-ray energy is given by:

$$E_{\gamma} = \frac{4\gamma^2 E_L}{1 + \gamma^2 \theta^2}. \quad (1)$$

$E_L$  is the laser quantum energy in keV and  $\theta$  is the emission angle in rad.

The yield of backscattered x-rays  $N_x$  into a cone of angle  $\theta_c$  is equal to [12]:

$$N_x = 2 \frac{N_e P_L L_L}{c A_{int} E_L} \sigma_c, \quad (2)$$

where  $N_e$  is the number of electrons in the electron bunch,  $P_L$  is the peak laser bunch power in W,  $L_L$  is the interaction length in m,  $E_L$  is in J ( $1 \text{ eV} = 1.602 \cdot 10^{-19} \text{ J}$ ),  $c$  is the speed of light in m/s,  $A_{int}$  is the interaction area in  $\text{cm}^2$  and  $\sigma_c$  is the Compton cross section in  $\text{cm}^2$  for photons scattered into a cone of angle  $\theta_c$ .

The laser-Compton scattering experiments were carried out at the Idaho Accelerator Center (IAC). The RF LINAC produces a 20-22 MeV electron beam that is brought to an approximate head-on collision with a pulsed 7 ns long, 10 Hz repetition rate and 100 MW peak power Nd:YAG laser. The Nd:YAG laser fundamental wavelength is equal to 1064 nm and the second harmonic is equal to 532 nm. This interaction generates two X-ray lines at 7.5 and 15 keV, respectively, when the observation direction coincide with the electron beam direction and for an electron beam energy equal to 20 MeV. The laser-pulse energies of the 1064 nm and 532 nm lines were 750 and 250 mJ respectively. A pair of slits located between two  $22.5^\circ$  bending magnets [9] enabled us to change the electron beam energy distribution as well as the electron beam current.

The experimental and optical setup is summarized in [9]. The Nd:YAG laser beam is first expanded to a 45 mm diameter beam and then focused by a 5 m focal lens. The lens focal point coincides with the center of the interaction chamber. An off axis  $45^\circ$  broadband mirror steers the laser beam toward the center of the interaction chamber. At the center of the interaction chamber, the laser beam spot size was equal to 0.12 mm for the 532 nm line. The angle between the Nd:YAG laser beam and the beam line

axis was equal to 4.65 mrad. The angle between the laser-beam and electron beam was about 1.6 mrad (see below).

The X-rays from the LCS passed through a 51  $\mu\text{m}$  thick Kapton window and traveled 1.8 m in air before reaching the liquid nitrogen cooled high resolution Si(Li) detector placed at  $0^\circ$  with respect to the beam line axis. The solid angle subtended by the detector was about  $0.68 \mu\text{sr}$  (1 sr is the solid angle of a sphere subtended by a portion of the surface whose area is equal to the square of the sphere's radius).

The lowest acceptable bremsstrahlung signal recorded was obtained when the electron beam is directed toward the broadband mirror. Most of the data were obtained when the angle between the electron beam and the beam line axis was about 3mrad. The electron beam was focused on the first actuator (upstream from the interaction chamber), and the laser beam was steered toward its center. At this position the laser beam spot size is approximately 3.4 mm. From this interaction geometry, the crossing angle was of the order of 1.6 mrad. The energy calibration and resolution of the Si-(Li) detector was determined by X-ray fluorescence from the bremsstrahlung X-ray beam hitting a 343  $\mu\text{m}$  thick Zr target and calibrated radioactive sources.

## EXPERIMENTAL RESULTS

### 1. Laser-Compton spectra

Once a clear LCS signal was detected, a time scan was performed. The goal of this time scan was to optimize the LCS X-ray yield as a function of the delay between the electron beam and laser pulses. In order to remove possible pile up from the 7.5 keV

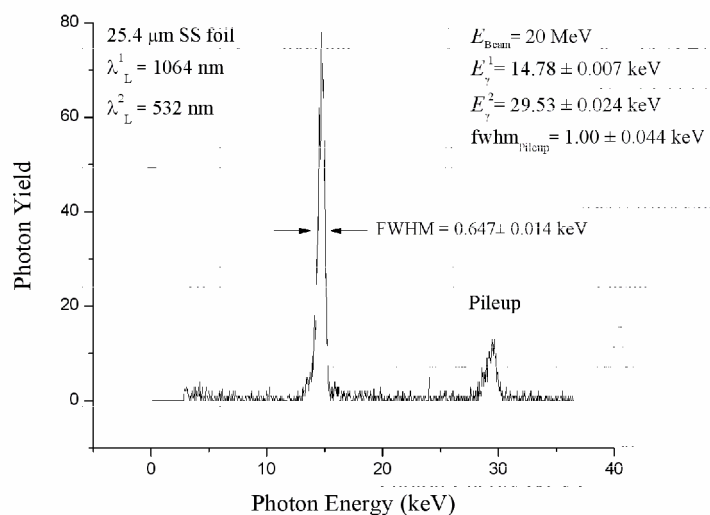


Figure 1. LCS spectrum using the Nd:YAG laser 532 line

X-ray resulting from the interaction of the electron beam with the 1064 nm laser line, a 25.4  $\mu\text{m}$  thick stainless steel (SS) foil was placed in front of the Si(Li) detector. The

X-ray transmission in air and SS foil for the 7.5 keV line was about 0.01% compared to 20% for the 15 keV line. Figure 1 shows the LCS spectrum for an observation angle equal to 3 mrad. The spectrum shows a clear sharp distinct monochromatic X-ray peak

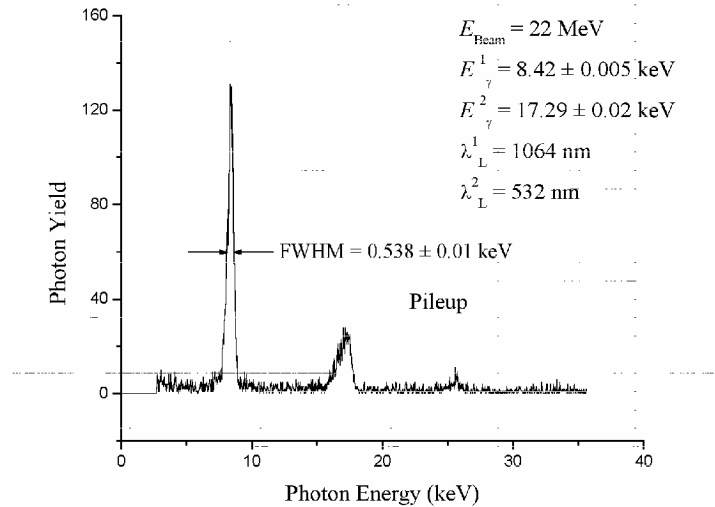


Figure 2. LCS spectrum using the fundamental and second harmonic laser lines.

resulting from the interaction of the 20 MeV electron beam with the 532 nm laser line on top of a low bremsstrahlung background. The additional higher energy peak is a result of a pile up from the major line. A  $25.4 \mu\text{m}$  thick SS foil was placed in front of the detector in order to block the X-rays from the interaction with the 1064 nm laser

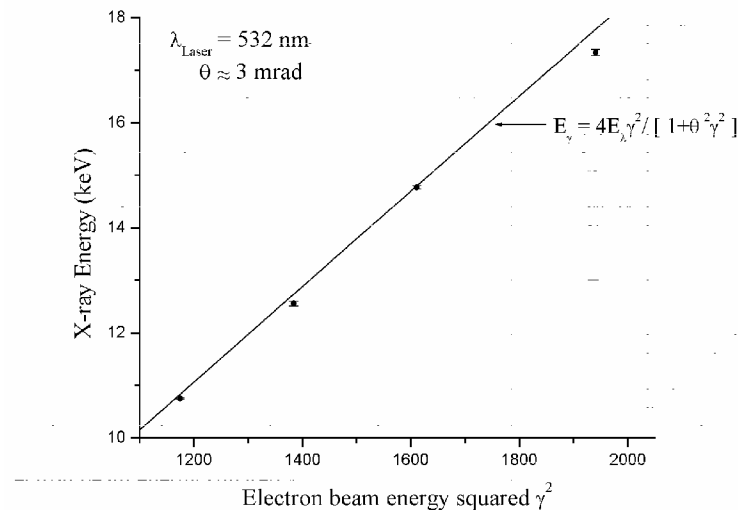


Figure 3. Second order LCS x-ray energy as a function of electron energy squared.

line. Figure 2 shows the LCS spectrum resulting from the interaction of a 22 MeV electron beam with the fundamental and second harmonic laser line. The peak located at 17.29 keV contains X-rays from the interaction with the second harmonic and

pileup from the fundamental line. The spectra in figures 1 and 2 were taken during different runs, and a change in beam direction causes the X-ray energies to be lower than expected at 22 MeV (see below). Figure 3 shows the photon energies as a function of the electron beam energy for the second order LCS together with Eq. 1 for an emission angle of 3 mrad. There is good agreement between the data collected and the theoretical predictions. The discrepancy observed for the electron energy equal to 22 MeV results from a change in the electron beam direction during beam tuning and therefore a change in the observation angle equal to 5 mrad.

## 2. Laser-Compton energy spread and Intensity

LCS energy spread depends on the energy spread of the laser  $\Delta E_L$ , the electron beam energy and angular spread  $\Delta E_B$ ,  $\Delta E_b^e$  and the spread of the scattering angle subtended by the detector  $\Delta E_\gamma^\theta$  [11]. In our experiment, the electron beam energy deviation, spot size and current are dominated by the width of the analyzing slits. The maximum electron beam current is recorded when the width of the slits is larger or equal to 3.5 cm. Figure 4 shows the variation of LCS energy spread, without detector resolution, as a function of electron beam energy deviation for an observation angle  $\theta$  equal to 3 mrad and X-ray energy equal to 14.75 keV. The upper x-axis in Figure 4 is the analyzing slits width and the lower x-axis is the corresponding electron beam energy spread. There is good agreement between experimental and predicted values. From this measurement, we see that the LCS width is solely determined by the electron beam energy deviation and that the additional contributions mentioned above are negligible. As the widths of the slits are increased, the electron beam spot size becomes comparable to that of the laser and LCS energy spread reaches a maximum and constant value.

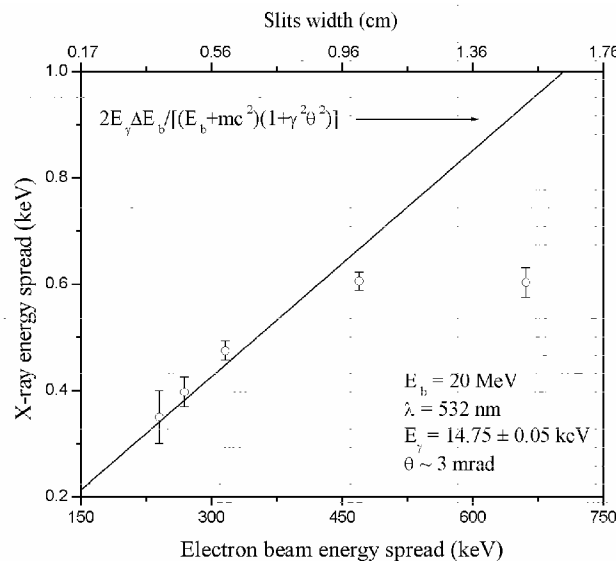


Figure 4. LCS natural energy spread as a function of the electron beam energy deviation. The electron beam energy spread was varied by changing the width of the 90° port slits [9]. The maximum slits width was about 5 cm.

The maximum X-ray yield registered during this experiment, for both X-ray lines emitted in a cone of opening angle  $1/\gamma$  is equal to  $3 \times 10^5$  photons/bunch which corresponds to an intensity of  $5.6 \cdot 10^{13}$  photons/s. This intensity is 3 orders of magnitude higher than the highest yield obtained from other x-ray sources involving electron beams interaction with periodic structures [7]. The brilliance obtained was about  $2 \cdot 10^{11}$  at 7.4 keV X-rays.

## CONCLUSION

LCS experiments using the head-on collision of a Nd:YAG laser and a 20-22 MeV electron beam were carried out at the IAC. Sharp monochromatic peaks with a low background were observed at different electron beam and laser energies. We have shown that there is a good agreement between experiment and theoretical predictions. We have also demonstrated the direct relation between measured LCS width and electron beam energy deviation. LCS X-rays flux can be further enhanced by several orders of magnitude by decreasing the interaction area and increasing the laser power [11].

This work partially funded by US Department of Energy under DOE Idaho Operations Office Contract Number DE-AC07-99ID13727.

## REFERENCES

- [1] H. Wiedemann et al., Nucl. Instr. and Meth. A 347 (1994) 515.
- [2] R. Carr, Nucl. Instr. and Meth. A 347 (1994) 510.
- [3] J. Freudenberger et al., Nucl. Instr. and Meth. A 466 (2001) 99.
- [4] H. Uberall et al., SPIE Proc. Short Wave Radiation Sources 1552 (1991) 198.
- [5] K. Chouffani et al., Nucl. Instr. and Meth. B 152 (1999) 479.
- [6] K. Chouffani et al., Nucl. Instr. Meth. B 173 (2001) 241.
- [7] R.O. Avakian et al., Nucl. Instr. Meth. B 145 (1998) 239.
- [8] W. P. Leemans et al., Phys. Rev. Lett. 77 (1996) 4182.
- [9] K. Chouffani et al., Nucl. Instr. and Meth. A 495 (2002) 95.
- [10] I. V. Pogorelsky et al., Nucl. Instr. and Meth. A 455 (2000) 176.
- [11] P. Sprangle et al., J. Appl. Phys. 72, (1992) 5032.
- [12] J. Stepaneck, Nucl. Instr. and Meth. A 412 (1998) 174.